

# Gelation and the production of stiff polyethylene fibres

P. J. Barham

H. H. Wills Physics Laboratory, University of Bristol, Tyndall Avenue, Bristol BS8 1TL, UK

(Received 12 August 1981; revised 5 March 1982)

The preparation of two sets of polyethylene fibres from the same solutions is described. One set is prepared by the surface growth technique and the other by drawing gels made from the solution. Some mechanical and physical properties and morphological studies of the two sets of fibres, and the undrawn gel are presented. Several conclusions can be drawn from these results. First the previous suggestion that the surface growth technique proceeds by the stretching out of gel particles adhering to the rotor surface is confirmed. Secondly a simple model, based on the observed fibre morphology and deduced structure of shish-kebabs, which can be used to predict the fibre mechanical properties is presented. Finally it is shown that by applying simple network theory to the observed mechanical behaviour of the gels the number of molecules in each network junction zone can be calculated to be approximately 20.

**Keywords** Gelation; polyethylene fibres; surface growth; gel drawing; morphology; mechanical properties; physical properties

## INTRODUCTION

There is at present considerable interest in the preparation of extremely stiff and strong polyethylene fibres by solution processing routes. This interest dates from the announcement by Zwijnenburg and Pennings<sup>1</sup> that they could grow fibres with stiffness up to 100 GPa and strength up to  $\sim 3$  GPa using their surface growth technique. Pennings and his co-workers have since published several more papers on this topic<sup>2-4</sup> and have arrived at the conclusion that the fibres are grown in an entanglement layer adsorbed onto the rotor surface. The surface growth technique was subsequently studied in this laboratory<sup>5</sup> and fibres with stiffness up to 140 GPa at room temperature (up to  $\sim 280$  GPa at  $-196^\circ\text{C}$ ) were grown<sup>6</sup>. In the course of these studies it was observed that the solutions from which fibres had been grown were prone to form gels on cooling; indeed a strong link was found between the ability of solutions to form fibres and their tendency to gel. It was deduced<sup>7,8</sup> that a layer of gel became adsorbed to the rotor surface and was stretched out to form the surface grown fibres.

Concurrently with this work Pennings *et al.* and Smith and Lemstra<sup>9-13</sup> were making gels of polyethylene and drawing them at elevated temperatures to produce fibres with similar properties to those prepared by the surface growth method. The gels have been drawn in a variety of ways, both before<sup>9-11</sup> and after<sup>12-13</sup> removing the solvent. However, no experiments have been performed which are directly comparable to the earlier work on the surface growth method.

The present work began with an attempt to produce a set of drawn gel fibres and a set of surface grown fibres under directly comparable conditions and to examine their structure and properties. In the course of this work new insights were gained into the structure of the polyethylene gel and of the shish-kebabs made by stretching it. In particular it was possible to produce a

very simple model which predicts the tensile modulus of the drawn gel fibres.

Hoffman has produced a theory for the formation of shish-kebabs by multiple nucleation on elongated chains<sup>14,15</sup> which introduces the concept of cumulative strain, such a model should also be applicable to the shish-kebabs formed by stretching of gels. Accordingly the results reported here are compared with Hoffman's theoretical predictions.

## EXPERIMENTAL DETAILS

### *Preparation of the drawn gel fibres*

*Preparation of the gels.* Gelation can be induced in high molecular weight polyethylene by stirring solutions at elevated temperatures and then cooling them to room temperature<sup>8</sup>. For this work sheets of gel were required from which samples could be cut for the drawing, and other experiments. Accordingly, solutions of the ultra-high molecular weight polyethylene, Hostalen GUR, were prepared in laboratory grade xylene at a nominal concentration of 0.75% (w/w). These solutions were then stirred, using the same apparatus used to prepare surface grown fibres, for 10 mins at 60 r.p.m. at  $115^\circ\text{C}$ . The stirred solutions were then poured into glass trays  $25\text{ cm} \times 4\text{ cm} \times 1\text{ cm}$  where the solutions formed into gels as they cooled; the gelation was encouraged by manually agitating the trays during cooling, this was done at a frequency  $\sim 0.5$  Hz with an amplitude  $\sim 5$  mm. The trays were covered with glass sheets to minimize evaporation of the solvent. During storage the gels underwent syneresis so that the trays eventually contained gels of dimension  $\sim 22 \times 3.5 \times 0.2$  cm surrounded by more or less pure solvent.

*Drawing of the gels.* The apparatus used to draw the gels is sketched in *Figure 1*; it consists of a rotor which is used

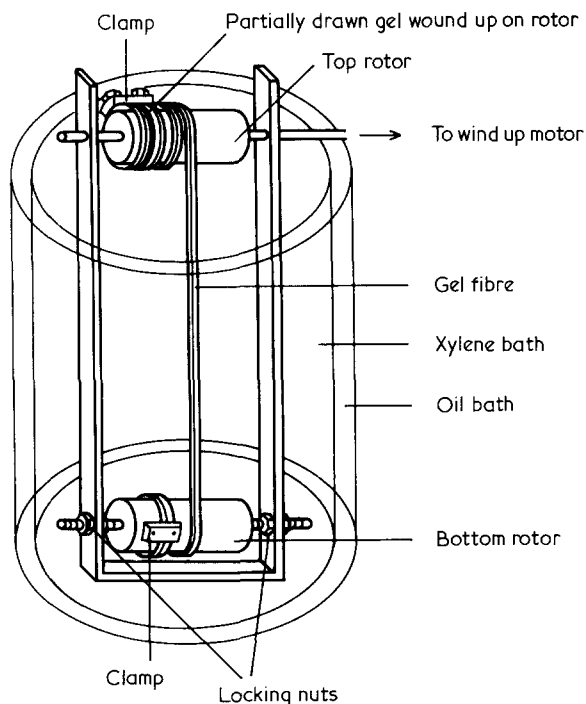


Figure 1 Sketch of the apparatus used to prepare drawn gel fibres

to draw a fixed length of gel at a constant strain rate. Strips 5 mm wide, 20 cm long were cut from the gel film, a 1 cm length of each strip was kept aside and used later to calculate the draw ratio. The solvent was removed from the two ends of the strip (this was done by squeezing the ends between filter papers) and the ends were then clamped onto rotors; one of the rotors was then clamped and lowered into a bath of hot xylene and the other fixed to a motor as shown in Figure 1. The gel was then allowed to reach thermal equilibrium by storage in the hot xylene for 10–20 mins before being drawn by being wound up onto the top rotor. The top rotor moved at a fixed surface speed of  $45 \text{ cm min}^{-1}$ . When the strip had been drawn the desired amount the motor was stopped and the whole assembly lifted out of the xylene. The central portion of the drawn gel fibre between the rotors was then clamped in a frame (to prevent longitudinal shrinkage) and cut away from the rotors; the drawn gel was then dried overnight at  $70^\circ\text{C}$  in a vacuum oven. No quantitative measurements of the amount of solvent remaining before, or after, drying were made. Measurements of weight loss showed that no further solvent would come off after 2–3 h in the vacuum oven. It was also found that the more highly drawn fibres showed very little weight loss on drying indicating the presence of very little solvent.

It is worth describing here the changes in the appearance of the gel during the various stages leading up to the drawing. When the solution is first poured into the glass tray at  $\sim 115^\circ\text{C}$  it is quite clear, it forms a clear gel as it cools below  $100^\circ\text{C}$ , this clear gel then becomes turbid and starts to shrink expelling solvent as it cools below  $\sim 80^\circ\text{C}$ . The shrinkage continues slowly as it cools to room temperature and the gel only reaches its final stable dimensions after  $\sim 1$  day at room temperature, (*n.b.* if the gel is not stored under solvent it will eventually dry out completely). When the gel is reheated in an excess of solvent it first swells a little until the temperature reaches  $\sim 90^\circ\text{C}$  when it becomes clear and quickly swells up to approximately its original dimensions, on further heating

the gel continues to swell slowly finally breaking up at  $\sim 120^\circ\text{C}$  to form a clear fluid. This clear fluid is not however a true solution since the gel will usually reform on cooling to  $\sim 100^\circ\text{C}$ ; only when the fluid is heated at, or above  $130^\circ\text{C}$  for some hours does it become a proper solution which gives rise to a single crystal suspension on subsequent cooling.

*The draw ratio of the gels.* The draw ratio of the gels could be measured in two ways. In the first method the draw ratio was taken to be the ratio of the dry weight per unit length of the undrawn to the drawn gel. The dry weight of undrawn gel was obtained from the 1 cm length cut from the original strip for this purpose, this was immersed in solvent at the drawing temperature for 15 mins before being dried overnight in a vacuum oven at  $70^\circ\text{C}$  and weighed. In the second method the draw ratio was calculated from the rotor speed and draw time (i.e.  $\lambda = 1 + \frac{v}{l_0}t$  where  $\lambda$  is the draw ratio,  $v$  the rotor surface speed,  $l_0$  the initial length of the gel and  $t$  the draw time). There was close agreement between the two methods, the second method nearly always giving draw ratios a few per cent higher than the first; this was attributed to slippage of the gel on the rotor during wind up. Accordingly only the measurements made by the first method are quoted here; some of these are presented in Figure 2 in the form of the maximum achieved draw ratio as a function of drawing temperature.

#### *The stiffness of the undrawn gel*

A specially prepared gel sample was mounted in an Instron tensile testing machine in a hot xylene bath so that the mechanical properties of the undrawn gel could be studied. The stiffness of the sample was measured as the temperature was increased, 20 mins were allowed between each experiment for the gel to reach thermal equilibrium.

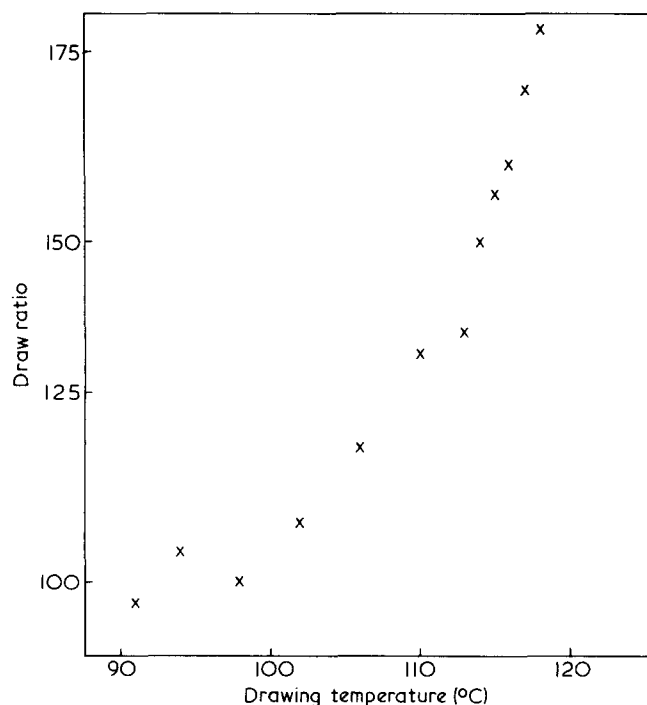


Figure 2 Graph showing how the maximum achievable draw ratio of polyethylene gels increases with drawing temperature

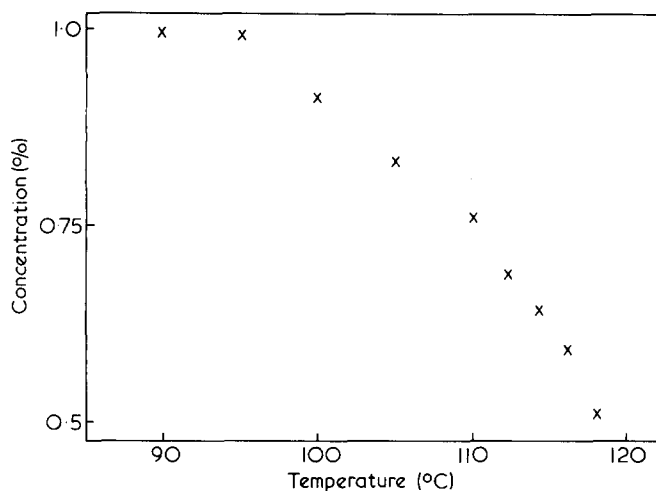


Figure 3 Graph showing concentration of the undrawn gel as a function of temperature during heating

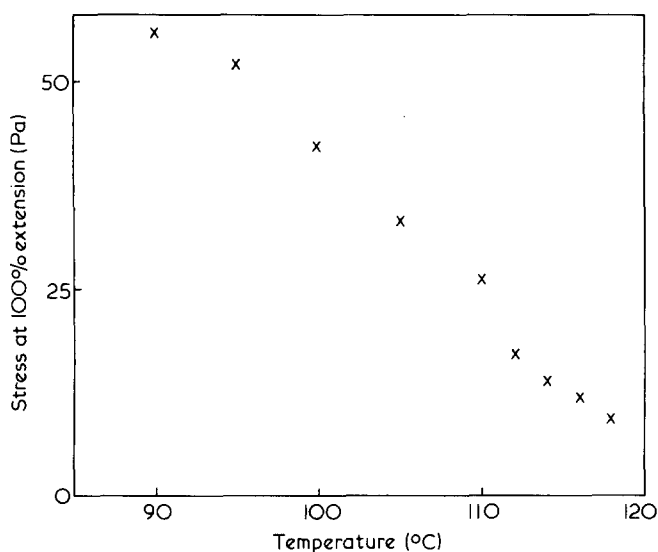


Figure 4 Graph showing how the stress required to impart a 100% extension to the undrawn gel varies with temperature

At each temperature the sample was extended from its length at zero load to double that length and then brought back to zero load again. The deformation rate used was  $1 \text{ cm min}^{-1}$ . After each experiment the specimen became longer; initially at  $90^\circ\text{C}$  the gel strip was 6.5 cm long at zero load and finally after 9 experiments at successively higher temperatures the length at zero load had increased to 8.1 cm. The lateral dimensions of the gel were measured using a travelling microscope. The gel swelled up considerably as the temperature was raised, this is illustrated in Figure 3 as a plot of gel concentration against temperature. Figure 4 shows how the stress (referred to cross section at zero load) required to produce an extension of 100% varies with the measurement temperature. The experiments were made at successively higher temperatures, no experiments were carried out on cooling because after the final experiment at  $118^\circ\text{C}$  the gel broke up.

#### Preparation of fibres by the surface growth technique

The surface growth technique of Zwiijnenburg and Pennings is well documented elsewhere<sup>1-5</sup>. The apparatus used in this work<sup>5</sup> consists in essence of a glass

cylinder of internal diameter 9.4 cm in which a PTFE cylinder of external diameter 8.2 cm is rotated. Fibres are grown from polyethylene solution at the surface of the PTFE rotor and are wound up outside the vessel. It is possible to vary the rotor speed and the fibre wind up speed independently and maintain growth over a range of conditions<sup>5</sup>. A number of fibres were grown using a variety of conditions but all were grown from aliquots of the same solutions used to make the gel sheets. All the surface grown fibres were washed in xylene at  $119^\circ\text{C}$  for 2 h to remove any excess polyethylene.

#### Modulus of the drawn gel and surface grown fibres

Tensile moduli of the fibres were measured using an Instron tensile testing machine at an initial strain rate of  $10^{-4} \text{ s}^{-1}$  and at a temperature of  $22^\circ\text{C}$ . The secant modulus at 0.1% strain is quoted here. The specimens all had sufficiently large aspect ratio ( $>200:1$ ) that end-effects could safely be ignored<sup>16</sup>.

The way in which the modulus of the dried gel fibres varied with draw ratio was first studied. In all cases there was a steady increase of tensile modulus with draw ratio, the rate of increase falling off as the maximum draw ratio was approached. This is illustrated in Figure 5 for fibres drawn at two different temperatures ( $110^\circ\text{C}$  and  $115^\circ\text{C}$ ). Next the way in which the modulus varied with drawing temperature was examined; it is clear from Figure 5 that there are several ways in which comparison could be made (e.g. modulus at a fixed draw ratio). However, the most meaningful measurement is probably the maximum achievable modulus (i.e. the modulus at the maximum draw ratio). A plot of the maximum modulus against drawing temperature is shown in Figure 6.

In a previous publication<sup>5</sup> it was stated that the modulus of the surface grown fibres depends primarily on the growth temperature, being little affected by the rotor and take-up speeds. It is important to the discussion to follow that the actual dependence of the fibre modulus on these variables is described here. Essentially the fibre modulus is independent of both rotor and take-up speeds except when they are slow in which case the modulus of the resulting fibre is reduced. It is difficult to achieve fibre growth at low rotor speeds owing to the frequency of breakages or at low take-up speeds since the fibre grows around the rotor to form a film<sup>17</sup>. The variation of modulus with take-up speed is illustrated in Figure 7a and with rotor speed in Figure 7b.

The moduli of the surface grown fibres (grown at take-up and rotor speeds in the plateau regions of Figures 7a

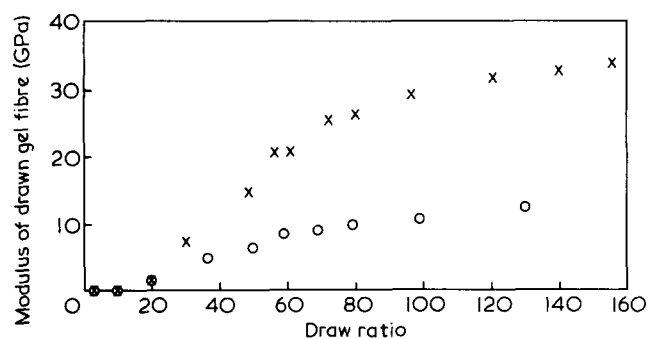


Figure 5 Graphs of modulus of drawn gel fibres against draw ratio (x – drawn at  $115^\circ\text{C}$ , o – drawn at  $110^\circ\text{C}$ )

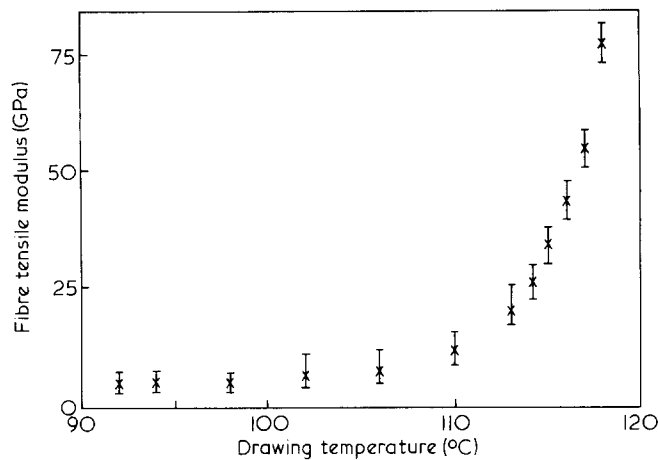


Figure 6 Graph of maximum modulus of drawn gel fibres against drawing temperature

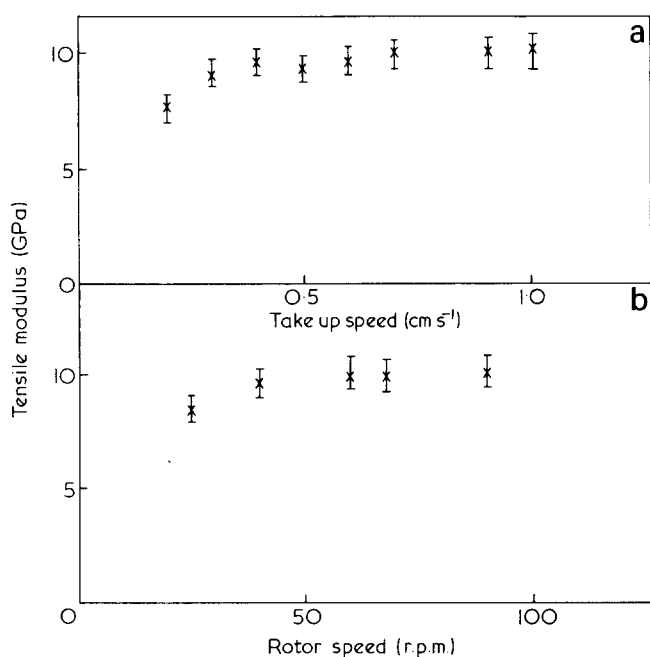


Figure 7 Graphs showing how the tensile modulus of surface grown fibres vary with (a) the take up speed, (b) the rotor speed. The temperature for both graphs is 110°C, the rotor speed in (a) was 60 r.p.m. and the take-up speed in (b) was 0.7 cm s<sup>-1</sup>

and 7b) were also measured; the results are presented, as a function of growth temperature, in Figure 8.

#### Thermal shrinkage of the fibres

Shish-kebab fibres have been observed to show a partially reversible shrinkage when heated close to their melting point<sup>18</sup>. Careful observations of this behaviour led to the conclusion that shrinkage was caused by the melting of crystalline segments in the shish-kebab cores, shorter crystals melting at lower temperatures. The reverse effects occurred when the molten short crystals recrystallized on cooling; due to the constraints on the ends of the molecules the crystals are forced to reform in their previous state thus causing elongation of the fibres. This leads to a model, for the structure of the shish-kebab core, of alternating crystalline, and short, non-crystalline regions, this is illustrated schematically in Figure 9. By using such a model and assuming a logarithmic distribution of crystal lengths, Grubb and Keller<sup>18</sup> were

able to fit the observed shrinkage-temperature behaviour using a single adjustable parameter, the mean crystal length. The parameter  $l$  in the distribution function  $w(l) = \frac{1}{\langle l^2 \rangle} \exp(-l/\bar{l})$  was in fact used by Grubb and Keller.

However, in this work the mean length ( $=2\bar{l}$ ) is used. It is worth noting here that in order to do the fitting, Grubb and Keller assumed that the diameter of the crystalline cores was 30 nm and that the end-surface free energy of the crystals was high (550 ergs cm<sup>-2</sup>). Such a high value of the end-surface free energy is supported by Hoffman<sup>15</sup> who

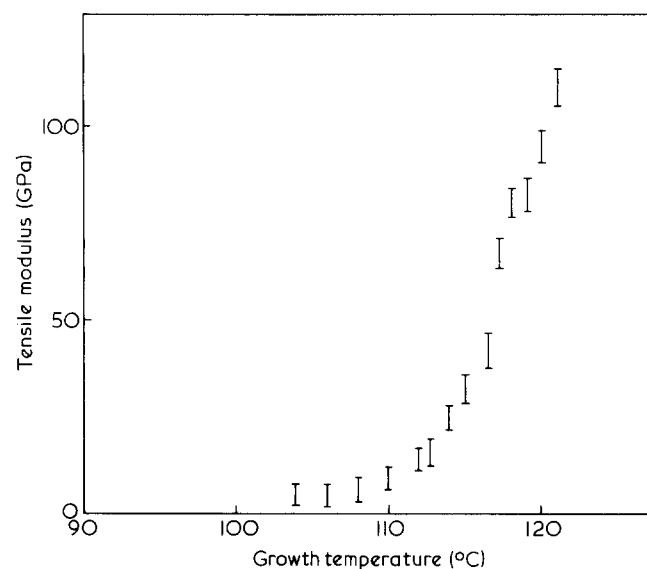


Figure 8 Graph of maximum modulus of surface grown fibres as a function of growth temperature

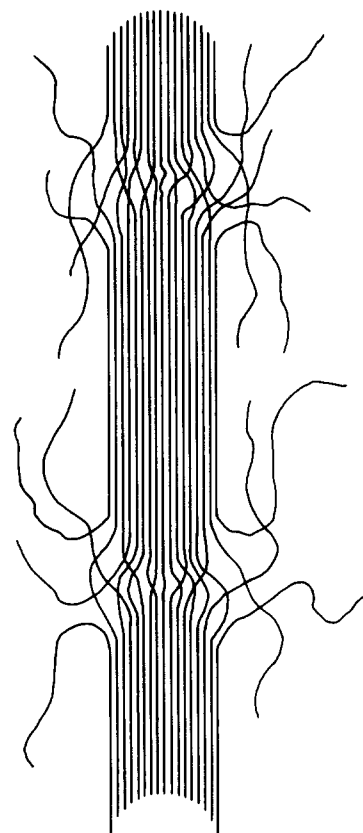


Figure 9 Sketch illustrating the Grubb-Keller model<sup>18</sup> for the structure of the central core of shish-kebabs

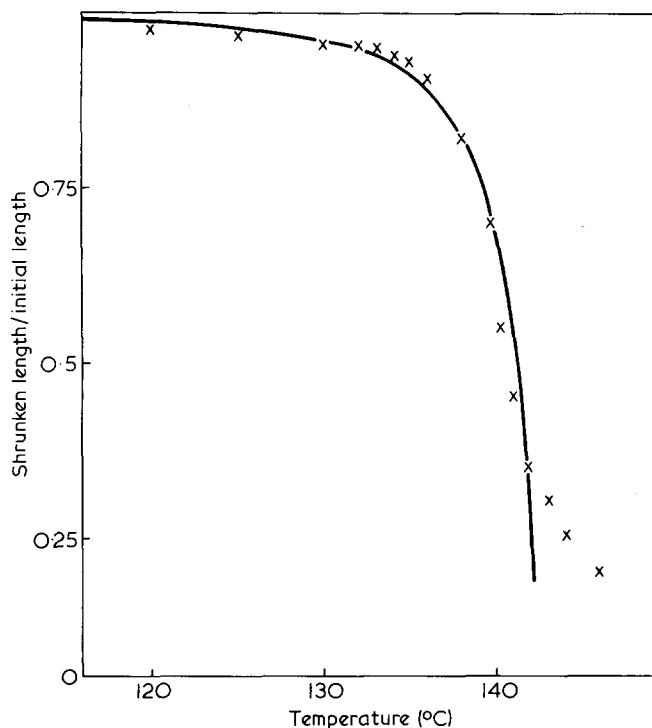


Figure 10 Graph showing the shrinkage of a drawn gel fibre on heating in silicone oil. The fibre was drawn at 106°C. The solid line shows the fit to the Grubb-Keller theory with a mean crystal length of 0.33  $\mu\text{m}$

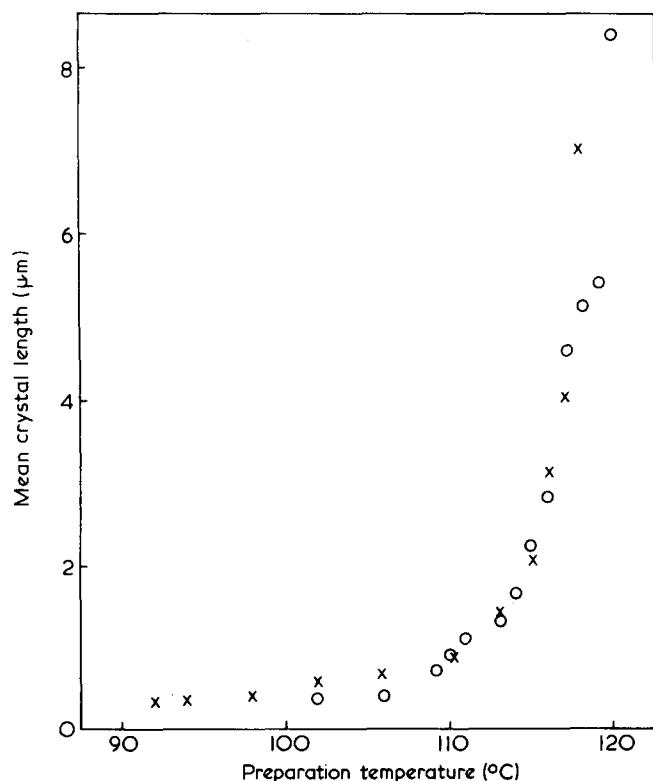


Figure 11 Graph showing how the mean crystal length derived from the Grubb-Keller model varies with the fibre preparation technique (x — drawn gel fibres, o — surface grown fibres)

argues that the strain caused by overcrowding at the crystal ends will significantly increase the surface energy.

The surface grown fibres and the drawn gel fibres show similar behaviour to that described above. Indeed the Grubb-Keller method has previously been used to

deduce mean crystal lengths in the cores of the shish-kebabs which make up the surface grown fibres<sup>19</sup>. The shrinkage behaviour of both sets of fibres used for modulus measurements (shown in Figures 6 and 8) was observed during heating in silicone oil at 0.2°C/minute. The data were then fitted to the Grubb-Keller model using the same values of the thermodynamic variables as they did, the core diameter was taken to be 30 nm in all cases. An example of one such fit is shown in Figure 10; and in Figure 11 the values of the mean crystal length obtained from the fitting procedure are plotted against the preparation temperature of the fibres (the drawing temperature for the drawn gels and the growth temperature for the surface grown fibres). It is clear that there is a strong correlation between the results for the two sets of fibres and that there is a systematic increase in mean crystal length as the preparation temperature is raised.

#### Electron microscopy

The appearance of the unoriented gels in the electron microscope has been reported previously<sup>8</sup>. The chief observation is of a very fine fibrous network on which very large platelet crystals which can be removed by washing are superimposed. Typical micrographs of unwashed and washed gels are reproduced in Figure 12. In these dried, unoriented gels only a small fraction of the material is seen to be involved in the fibrous network. When the drawn gels are examined a very different state of affairs is seen.

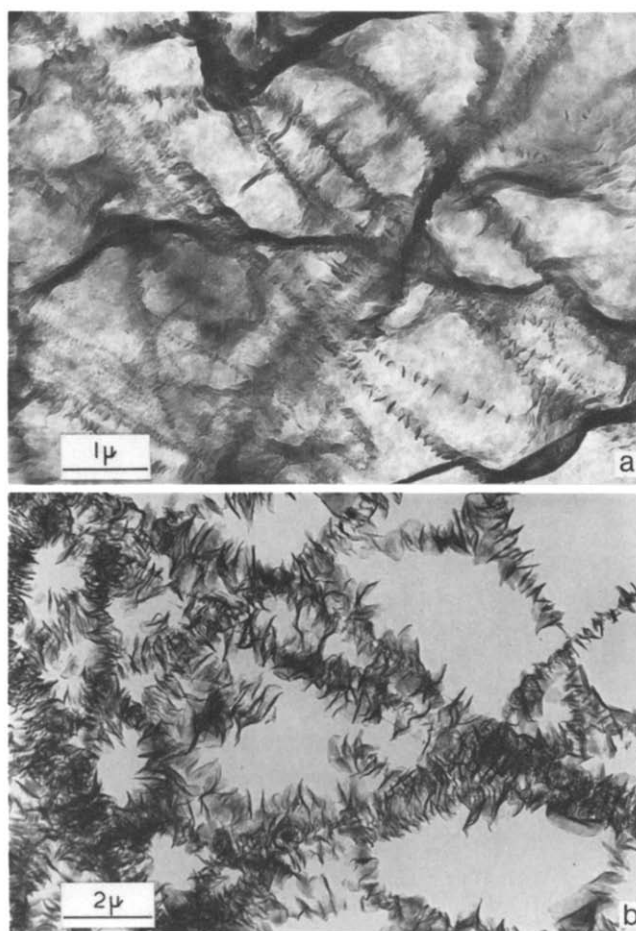


Figure 12 Typical micrographs of dried gels (a) unwashed, (b) after washing at 119°C followed by recrystallization at 96.7°C



Figure 13 Typical micrograph of a drawn gel fibre, drawn at 117°C and subsequently washed at 114°C

The specimens appear as films of aligned shish-kebab like fibres. Figure 13 shows a typical micrograph, there is no significant change of appearance on washing.

The essential differences between the undrawn and drawn gels are, first that the fibrous network becomes oriented into a parallel array of shish-kebabs and secondly that either virtually all the molecules in the gel are transformed into the shish-kebab morphology on drawing, or a large proportion of the polymer molecules are expelled from the gel during drawing, which has not been observed.

In addition to looking at morphology it is possible to estimate the proportion of material in the central thread, and the diameter of the central thread from the micrographs. This has been done for several specimens and the results vary from micrograph to micrograph. The best estimate of the proportion of material in the central thread is 30–40% and of the core diameter is 25–30 nm. There is no evidence to suggest any variation in either of these with the formation temperature of the shish-kebabs; however since measurements of both parameters vary over a single preparation no firm conclusion can be drawn.

## DISCUSSION

The results of this work, originally intended to establish once and for all the links between gelation and the surface growth method, have led to a number of interesting observations from which useful deductions can be made. These will all be discussed separately. In the first part of the discussion the equivalence of the two sets of fibres is shown to be well established and the structure of the gel prior to drawing, and its subsequent transformation into shish-kebabs on drawing, is discussed.

### *The structure of the gels*

The surface growth method allows fibres to be grown, at very high temperatures, from dilute solution, indeed it is possible to grow fibres at temperatures above the

usually quoted dissolution temperature. The fibres have been seen to grow in a layer of solution adhering to the rotor surface<sup>5</sup>, Barham, Hill and Keller<sup>8</sup> have previously concluded that this layer is an adsorbed gel layer. This conclusion was reached as a result of studies of the conditions under which solutions would support surface growth and of the conditions which led to gelation on subsequent cooling. It was found that only those solutions which would form gels on subsequent cooling were capable of supporting fibre growth at the rotor surface. The conclusion was supported by evidence showing an accumulation of polyethylene at the rotor surface during stirring, and by electron micrographs of the dried gel which showed a shish-kebab type of morphology. Further, it was argued that the work of Smith *et al.*<sup>9</sup> which showed that fibres with high tensile modulus and strength, comparable with those of surface grown fibres, could be produced by stretching wet, or dried out gels, gave added support for the conclusion. There was, however, no more direct evidence concerning the fibres drawn from the gel state which could be compared with fibres prepared by the surface growth method.

The preparation and properties of two sets of fibres made from the same polyethylene solutions have been described above: the first set being drawn directly from the gel state and the second being made using the surface growth technique. According to the previous conclusions<sup>7,8</sup> the two sets of fibres should be virtually indistinguishable. Indeed the measurements of fibre modulus, shown in Figures 6 and 7, show that the maximum modulus which can be achieved at any preparation temperature is closely similar for the two types of fibre. In the surface growth method the fibre is stretched as it is wound up; the amount of stretching will of course be reduced at low take-up or rotor speeds. This reduction in the degree of stretching of the fibre during growth and subsequent wind-up is reflected in the observations of reduced tensile modulus at low take-up or rotor speeds shown in Figure 7. A similar variation of modulus with the degree of stretching (draw ratio) is also observed for the drawn gel fibres and is shown by the plot of modulus against draw ratio in Figure 5. The shrinkage behaviour of the two sets of fibres and the inferred mean crystal lengths shown in Figures 10 and 11 are very similar and also correspond to those previously reported for surface grown fibres<sup>19</sup>. The electron micrographs of drawn gel fibres show a shish-kebab fibrous appearance as do electron micrographs of surface grown fibres (see e.g. ref. 19).

Thus no major distinctions can be drawn between the physical properties of the drawn gel and surface grown fibres prepared at the same temperature. This gives ample support to the original suggestion that the surface growth method proceeds via the stretching of a gel at the rotor surface.

Now let us consider the structure of the gel prior to drawing. The most obvious and surprising property of the unoriented polyethylene gels is that they exist at all. Normally, on cooling a polyethylene solution the formation of single crystals (or aggregates of single crystals) is observed. Indeed at room temperature xylene is such a poor solvent that the polyethylene is expected to be fully crystalline. Nevertheless it is possible to make polyethylene gels which retain 90–95% by volume of solvent at room temperature. These gels may be stored

Table 1 Number of junctions and segments in the gel network

Temperature (°C)	No. of segments/m <sup>3</sup> from equation (1), $N_s$	Max. extensibility $\lambda_{\max}$ from Figure 2	No. of junctions/m <sup>3</sup> from equation (5)	$2N_s/N_j$ no. of chains/junction
90	$6.6 \times 10^{21}$	94	$6.2 \times 10^{20}$	21
95	$5.9 \times 10^{21}$	98	$5.4 \times 10^{20}$	22
100	$4.8 \times 10^{21}$	104	$4.6 \times 10^{20}$	21
105	$3.6 \times 10^{21}$	114	$3.5 \times 10^{20}$	21
110	$2.9 \times 10^{21}$	130	$2.3 \times 10^{20}$	25
112	$1.9 \times 10^{21}$	140	$1.9 \times 10^{20}$	20
114	$1.5 \times 10^{21}$	150	$1.5 \times 10^{20}$	20
116	$1.3 \times 10^{21}$	160	$1.2 \times 10^{20}$	22
118	$1.0 \times 10^{21}$	178	$0.9 \times 10^{20}$	22

indefinitely without visibly changing their properties, providing the solvent is not allowed to evaporate. If the solvent is allowed to evaporate then the resulting dry solid will not swell up again, to any significant extent, if reimmersed in solvent at room temperature. It therefore appears that at room temperature the gel remains stable, i.e. some molecules or parts of the molecules remain solvated until the solvent is removed, then they may crystallize. Normally it would be expected that such crystallization would take place with the solvent present; indeed some such crystallization probably does occur as the gel synergizes to an equilibrium concentration, as described above in the section on preparation of the gels. The question to be answered in this case is then, what mechanisms allow the retention of so much solvent at room temperature?

On the other hand the gel is also remarkably stable at high temperatures. On heating the gel, in excess solvent, it becomes clear at  $\sim 90^\circ\text{C}$  (this is associated with the dissolution of chain folded platelet crystals) and then it becomes progressively softer and more fragile, until it finally disintegrates at a temperature of approximately  $119^\circ\text{C}$ . However if the solution is then cooled from any temperature up to  $\sim 130^\circ\text{C}$  the gel will usually reform when the temperature has dropped to  $\sim 100^\circ\text{C}$ ; reformation of the coherent gel is greatly aided by very gentle stirring as reported previously<sup>8</sup>. Thus the gel forming structure remains stable at temperatures well above the equilibrium dissolution temperature, although the gel itself 'melts' at about that temperature. The problem in this case resolves itself into the questions of what is the gel forming structure? And why is it more stable than normal crystalline polyethylene?

It is possible to speculate on the nature of the solvent trapping mechanisms in the cold gel. The electron micrographs of thin films of dried gels<sup>8</sup> reveal an underlying fibrous network with large platelet crystals superimposed. At one extreme one could envisage that in the wet gel state, prior to drying, there were many tie molecules running between the fibres of the network. Such molecules would only be able to crystallize if the fibrous network were to collapse. Thus as long as the network of fibrils is held apart either by the presence of the solvent, or by tension in other tie molecules, the tie molecules will remain in solution. In other words if the energy to be gained by crystallizing these molecules is less than that required to pump the solvent out of the network, then the system will retain its solvent. An additional driving force, e.g. the evaporation of solvent due to a concentration gradient, is then required before the tie molecules can crystallize. At the other extreme a system of partially

closed cells formed by the platelet overgrowth crystals could be envisaged; the solvent now being trapped in these cells which will only collapse if, and when the solvent is removed (e.g. by evaporation). In this case the stability of the gel at room temperature would be due to the formation of closed cells by the large platelet crystals; a structure resembling a sponge. After drying, the cells would collapse and the interactions between crystal surfaces would prevent substantial reswelling.

In practice of course both these solvent trapping mechanisms may be expected to contribute to the stability of the gel at room temperature.

Some insights into the structure of the gel at high temperatures may be gained from a consideration of the mechanical properties of the gel. If it is assumed that the gel behaves, at high temperatures, as an entropy elastic network, it is possible to make some simple calculations. The simplest expression for the stress in a rubber-elastic network under uniaxial tension is

$$\sigma = N_s k T \left( \lambda - \frac{1}{\lambda^2} \right) \quad (1)$$

where  $\sigma$  is the stress,  $N_s$  the number of network segments per unit volume,  $k$  Boltzmann's constant,  $T$  the absolute temperature and  $\lambda$  the extension ratio. There are of course many assumptions hidden in equation (1) which have been considered in treatises on rubber elasticity. In what follows however, the simple expression of equation (1) will be used since it is only realistic to consider 'order of magnitude' estimates here. It is possible to calculate  $N_s$  using the data on stress at 100% extension ( $\lambda = 2$ ) given in Figure 4. The results of such calculations are presented in Table 1, it can be seen that the number of network segments decreases as the temperature is raised.

Further information can be obtained from a consideration of the large scale deformation of a network. If the chain segments connecting the junctions adopt random coil dimensions then their root mean square end to end distance,  $\langle \bar{r}^2 \rangle^{\frac{1}{2}}$ , will be

$$\langle \bar{r}^2 \rangle^{\frac{1}{2}} = n_e^{\frac{1}{2}} l_e \quad (2)$$

where  $l_e$  is the length of one chain link and  $n_e$  the number of such links between junctions. Equation (2) only holds for a freely jointed chain, for real chains an equivalent link is defined such that both equation (2) and the condition that the length  $l$  of the fully extended chain is given by

$$l = n_e l_e \quad (3)$$

Table 2 Contour length of network segments

Temperature (°C)	Contour length (μm)	
	From equation (6)	From equation (7)
90	11	8
95	12	9
100	14	10
105	16	12
110	21	14
112	25	20
114	28	23
116	32	24
118	40	28

are satisfied. For polyethylene the equivalent link has a length of  $\sim 1.3 \text{ nm}^{20}$ . When such a network is deformed the maximum deformation ratio,  $\lambda_{\text{max}}$  will be

$$\lambda_{\text{max}} = \frac{l}{\langle \bar{r}^2 \rangle^{1/2}} = n_e^{1/2} \quad (4)$$

The measured draw ratios shown in *Figure 2* may be assumed to reflect the maximum extensibility of the gel network, since the modulus of the fibres increases continuously with draw ratio. In addition, in a separate study of dried gels, Cannon<sup>21</sup> has found that the birefringence increases continuously with draw ratio. From a knowledge of the maximum achievable draw ratio  $\lambda_{\text{max}}$ , the number of equivalent links between junctions,  $n_e$  and hence the number of junctions per volume  $N_j$  may be calculated, assuming that the links form a lattice without any interpenetration.

$$N_j = \frac{1}{n_e^{3/2} l_e^3} = \frac{1}{\lambda_{\text{max}}^3 l_e^3} \quad (5)$$

The values of  $\lambda_{\text{max}}$  extrapolated from *Figure 2* and the values of  $N_j$  calculated from them are included in *Table 1*. The values of  $N_s$ , the number of network segments per unit volume range from  $\sim 10^{20}$  to  $\sim 7 \times 10^{21} \text{ m}^{-3}$  while the number of junctions,  $N_j$  range from  $\sim 10^{20}$  to  $\sim 6 \times 10^{20} \text{ m}^{-3}$ . Since each network segment must have each end in a junction, the number of molecules in each junction is at least  $2N_s/N_j$ . This ratio, which is also given in *Table 1*, is always  $\sim 20$  implying that the junctions all contain at least 20 chains.

This model is of course oversimplified, but is probably not too far from reality for the very dilute concentrations used in this work. From a knowledge of the number of junctions per unit volume and the concentrations, it can be seen that 20 chains/junction would imply that  $\sim 90\%$  of the chains are involved in the gel network. At first sight this might seem to be in conflict with the observation that, on the shish-kebabs arising from drawn gels only  $\sim 30\%$  of the polymer is in the central core. However when it is recalled that the material not in the central core is, nevertheless, intimately attached to it and consists primarily of loose loops and hairs it can be seen that there is no problem in allowing  $90\%$  of the chains to be involved in the network.

The validity of the foregoing arguments can be tested by a consideration of the contour length,  $l_s$ , of the network segments between the junctions. This can be obtained from the maximum achievable draw ratio using equation

(4) so that

$$l_s = n_e l_e = \lambda_{\text{max}}^2 l_e \quad (6)$$

$l_s$  can also be obtained from a consideration of the number of network segments/unit volume, and the total contour length of molecules in the network/unit volume,  $L_c$  (which can easily be found from the concentration) as

$$l_s = \frac{L_c}{N_s} \quad (7)$$

values of  $l_s$  calculated from both equations (6) and (7) are given in *Table 2*. There is a good correlation, the values calculated from equation (7) always being a little lower. The range of values of  $l_s$  is from  $\sim 10 \mu\text{m}$  at  $90^\circ\text{C}$  to  $\sim 40 \mu\text{m}$  at  $118^\circ\text{C}$ ; this corresponds to a molecular weight between junctions of  $\sim 10^6$  at  $90^\circ\text{C}$  and  $\sim 4 \times 10^6$  at  $118^\circ\text{C}$ . The weight average molecular weight of the Hostalen GUR polymer used in this work is quoted as  $1.2 \times 10^6$ , although this was not checked for the particular batch used it is probably a reasonable figure. Thus although the values of the molecular weight of the network segments calculated above are high they are by no means impossible. It is reasonable to suggest that only the longest molecules are involved in the network, shorter molecules being expelled into the surrounding solvent so that the molecular weight of the actual polymer in the gel network would be somewhat higher than that of the original batch. The fact that the segment length increases with the temperature suggests that the reason for the break up of the gel at  $\sim 119^\circ\text{C}$  is that there are insufficient very long molecules (molecular weight  $> 4 \times 10^6$ ) present to hold it together. The evidence that the gel will reform on cooling suggests that the junction zones themselves are not destroyed during heating. One possible explanation would be that during heating the least stable molecules associated with each junction become detached thus removing some junctions or groups of junctions from the network. At sufficiently high temperatures the network would no longer persist throughout and the gel would break up. On cooling some molecules would recombine with the junctions so that the gel is reformed.

There are several implications of the deduction that there are  $\sim 20$  chains (at least) in each junction. First, and most obvious, is the fact that such a high number cannot be accounted for simply by entanglements. The junction zones must therefore be some sort of molecular aggregate; it is interesting to speculate as to the nature of such aggregates. The least unlikely possibility is one of crystalline junction zones, but they would need to have a very high dissolution temperature; remember that the gel will still reform even after heating at  $130^\circ\text{C}$  for several hours. A possible, but unlikely, cause of a high melting point would be that the crystals were constrained by the network tie molecules so that they could not dissolve, a situation analogous to the appearance of a very high melting point hexagonal phase in constrained surface grown fibres<sup>2</sup>. If the junction zones are not polyethylene crystals is it more difficult to explain the observations; three possibilities will be examined. First the junctions may be caused by physical adsorption of the molecules onto foreign particles (perhaps nucleating agents)



suspended in the solutions. The principal drawback of this is that a wide variety of polyethylenes from different sources can be caused to gel in a variety of solvents, one would not expect to find similar suspended particles in each case. Secondly, there is the possibility that the polyethylene chains may have defects (e.g. sequences of methyl branches, giving rise to a sequence of polypropylene) which can cocrystallize in a crystal with higher stability than is normal for polyethylene; again this has the problem that a wide variety of high molecular weight polyethylenes can be caused to gel. Thirdly there is the possibility of liquid crystalline junctions, although there is no good reason why they should be stable at such low concentrations.

To summarize, the assumption that the gel behaves as an entropy elastic network is entirely self-consistent and leads to the conclusion that there are highly stable junction zones which contain up to 20 chains each.

#### Tensile modulus of the fibres—a model

All the fibres, no matter how they were prepared, have a shish-kebab microstructure. The presently accepted model of shish-kebabs is the one described above, in the section on thermal shrinkage, and sketched in *Figure 9* where the central thread consists of long crystals with disordered regions at their ends where molecules can leave the core or join the next backbone crystal in a different lattice position. These molecular segments which leave the core crystallize epitaxially on to the core on cooling, to give the usual overgrown platelets seen in the electron microscope. When there are many cores close together the platelet overgrowths are often seen spanning several cores.

The fibres prepared at high temperatures have high tensile moduli and long crystals in the shish-kebab cores. This correlation between crystal length in the backbone and tensile modulus suggests that the crystalline regions of the shish-kebab cores act rather like reinforcing fibres in a short fibre composite material; longer reinforcing elements having better stress transfer characteristics and hence leading to higher composite moduli. In the analysis that follows the crystalline regions of the shish-kebab cores will be identified with the reinforcing phase and the platelet overgrowths, together with any non-crystalline material, will be identified with the matrix phase. It should be borne in mind that there may be many small defects in the shish-kebab cores which, while breaking true crystal symmetry, do not significantly affect thermal or mechanical properties<sup>22</sup>. For the purpose of this analysis then, the lengths of the crystalline regions of the core are the same as those found from the shrinkage data.

Probably the simplest approach to describe the overall modulus of a composite of aligned short stiff fibres in a soft matrix is shear-lag theory<sup>23</sup>. This theory assumes that no stress is transferred across the ends of the reinforcing fibres, that there are no normal stresses, that all the reinforcing fibres have the same shape and size, are perfectly aligned and packed on a hexagonal lattice. It also assumes that both phases are homogeneous and isotropic. While it cannot be claimed that any of these assumptions will be valid for fibres consisting of arrays of shish-kebabs it is possible to justify most of them. The assumption that there are no normal stresses should be reasonable, since the Poisson's ratio of the overgrowths in the matrix phase and the crystals in the reinforcing phase

should be the same. The stress transferred across the ends of the shish-kebab core crystals will be small provided that there is a large disruption of the crystal lattice (which is to be expected) and that the crystals have a high aspect ratio, which in general they do. Wide angle X-ray diffraction patterns of the fibres show that there is near perfect *c*-axis orientation. In a study of the drawing behaviour of polypropylene<sup>24</sup> it was shown that neither the introduction of a distribution of lengths of the reinforcing elements nor, from finite element calculations, the introduction of anisotropic reinforcing elements make a major difference to the results of shear-lag theory. The simple shear-lag theory is therefore used with the assumptions that it is permissible to take an average matrix stiffness for the overgrowths and amorphous regions and ignore the effects of anisotropy and end-loading. The basic equations of shear-lag theory are:

$$E_c = cE_f \left(1 - \frac{\tanh x}{x}\right) + (1-c)E_m \quad (8)$$

where

$$x = \frac{l}{r} \sqrt{\frac{G_m}{E_c \ln\left(\frac{2\pi}{3c}\right)}} \quad (9)$$

$E_c$  is the composite tensile modulus,  $E_f$  the tensile modulus of the reinforcing elements,  $E_m$ ,  $G_m$  the tensile and shear moduli of the matrix,  $c$  the concentration of the reinforcing phase,  $l$  the length and  $r$  the radius of the reinforcing elements.

The modulus and thermal shrinkage measurements on both sets of fibres give a total of 26 independent pairs of modulus and crystal length values, which may be used to test the model. If equation (8) is rewritten as:

$$E = c_1 \left(1 - \frac{\tanh c_2 l}{c_2 l}\right) + c_3 \quad (10)$$

then a good fit is found when  $c_1 = 128$  GPa,  $c_2 = 4.24 \times 10^5$  m<sup>-1</sup> and  $c_3 = 4.8$  GPa. This is illustrated in *Figure 14* by a plot of modulus against crystal length on which the line defined by equation (10) is also drawn. In the section on electron microscopy it was stated that a good value for the

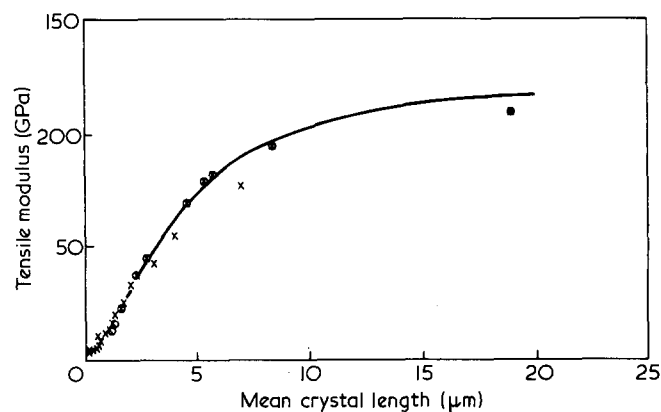


**Figure 14** Graph of tensile modulus of the fibres against mean crystal length (X drawn gel fibres, O — surface grown fibres). The solid line comes from the theory given by equation (10)

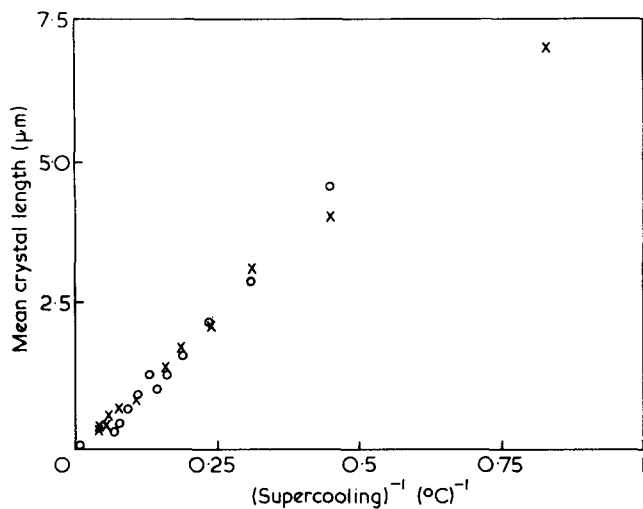


Figure 15 Graph of mean crystal length derived from the Grubb-Keller model against inverse supercooling; the dissolution temperature was taken to be 119.8°C. (x — drawn-gel fibres, o surface grown fibres)

proportion of the material in the shish-kebab cores was approximately 40%, and that this was more or less independent of the preparation temperature. From equation (8) it can be seen that  $c_1 = cE_f$  and  $c_3 = (1 - c)E_m$  so, using  $c = 0.4$ ,  $E_f$  is found to be 320 GPa and  $E_m$  is 8 GPa. These figures are not at all unreasonable. There are many values for theoretical crystal modulus of polyethylene in the literature varying from ~250–380 GPa<sup>25–27</sup>. The value obtained by Wobser and Blasenbury<sup>26</sup> is in fact 320 GPa, however it would be most unwise to draw any conclusions from this coincidence.

The fit to the model relies on evidence from two sources—mechanical measurements on the fibres themselves, and the crystal lengths deduced from shrinkage data. The fit does not depend on the absolute values of crystal length, merely on their relative values. The Grubb-Keller model should, despite the many assumptions implicit in it, give a reliable estimate of the relative values of mean crystal length in a variety of samples. The fact that such a good fit, as shown by Figure 14, can be obtained for such a simple and approximate model suggests that the underlying principle of the model, that the crystalline regions in the shish-kebab backbones act as reinforcing agents in a matrix consisting of the platelet overgrowths and any amorphous material, is probably correct.

#### Hoffman's theory for the formation of shish-kebabs

Hoffman has proposed a theory of flow induced fibril formation in polymer solutions<sup>14,15</sup>. He suggests that multiple nucleation events occur among the elongated molecules producing an embryonic fibril that is a connected set of bundle-like nuclei. The chains in the non-crystalline zones between these nuclei or crystallites exert a lateral force on the bundle ends which builds up as the crystallites grow, leading to a high surface free energy and to a volume strain in the as grown crystallites. The theory predicts that there will be a stable crystalline length and diameter, achieved when the extra volume strain introduced by further crystallization becomes prohibitively large. The overall treatment leads to a structure for the shish-kebab cores which is closely similar to that proposed by Grubb and Keller<sup>18</sup> and sketched in

Figure 9. The same theory should be applicable to chains elongated by stretching a gel as well as those elongated by flow, especially since the resulting fibres are in both cases shish-kebabs.

The principle predictions of the theory are that both the length,  $l$ , and the diameter,  $a$ , of the crystalline regions of the shish-kebab cores should be proportional to the inverse of the supercooling, so that

$$l = \frac{c\sigma_{e0}}{\Delta T}; \quad a = \frac{c\sigma}{\Delta T} \quad (11)$$

where  $c$  is a constant,  $\sigma_{e0}$  is the end surface free energy of an unstrained crystal,  $\sigma$  the side surface free energy and  $\Delta T$  the supercooling.

If the data (at temperatures below 119°C) in Figure 11 are replotted in the form  $l$  against  $1/\Delta T$ , taking the equilibrium dissolution temperature to be 119.2°C, then a linear relationship is indeed found, as shown by Figure 16. However, the electron microscopy data show no significant variation in the core diameter with growth temperature.

It is therefore apparent from the measurements reported here that Hoffman's theory of shish-kebab growth has successfully predicted the variation of the length of the crystalline regions in the core with preparation temperature. However the theory in its present form does not predict the observed core diameter.

## CONCLUSIONS

Several conclusions can be drawn from this work; first the previous suggestion<sup>7,8</sup> that the surface growth technique proceeds *via* the deformation of a polymer gel built up at the rotor surface has been confirmed. Secondly, the Grubb-Keller model of the shish-kebab core structure<sup>18</sup> not only explains the thermal shrinkage behaviour but can also be used, in conjunction with shear-lag theory, to predict the tensile modulus of an array of shish-kebabs. Thirdly, Hoffman's multiple nucleation theory of shish-kebab formation<sup>14,15</sup> accurately predicts the variation of crystalline sequence length in the shish-kebab core, although in its present form it does not predict the core diameter. Finally, some light has been thrown on the structure of the polyethylene gels, in particular it has been shown that there are extremely stable junction zones each of which contain some 20 chains.

## ACKNOWLEDGEMENTS

I wish to thank Dr Mary Hill for the electron micrographs of Figures 12 and 13; to thank Professor A. Keller and Mr C. G. Cannon for helpful discussions, and to thank ICI for financial support.

## REFERENCES

- 1 Zwijnenburg, A. and Pennings, A. J. *Colloid Polym. Sci.* 1976, **254**, 868
- 2 Zwijnenburg, A. *Ph.D. Thesis*, University of Gröningen (1978)
- 3 Pennings, A. J. and Torfs, J. *Colloid Polym. Sci.* 1979, **257**, 547
- 4 Zwijnenburg, A. and Pennings, A. J. *J. Polym. Sci., Polym. Phys. Edn.* in press
- 5 Barham, P. J. and Keller, A. *J. Mater. Sci.* 1980, **15**, 2229
- 6 Barham, P. J. and Keller, A. *Polym. Lett.* 1979, **17**, 591

**Gelation and production of polyethylene fibres: P. J. Barham**

- 7 Barham, P. J. *Disc. Faraday Soc.* 1979, **68**, 484
- 8 Barham, P. J., Hill, M. J. and Keller, A. *Colloid Polym. Sci.* 1980, **258**, 899
- 9 Smith, P., Lemstra, P. J., Kalb, B. and Pennings, A. J. *Polym. Bull.* 1979, **1**, 733
- 10 Smith, P. and Lemstra, P. J. *J. Mater. Sci.* 1980, **15**, 505
- 11 Smith, P. and Lemstra, P. J. *Colloid Polym. Sci.* 1980, **258**, 891
- 12 Kalb, B. and Pennings, A. J. *Polymer* 1980, **21**, 3
- 13 Snook, J., Torfs, J. C., van Hutton, P. M. and Pennings, A. J. *Polym. Bull.* 1980, **2**, 293
- 14 Hoffman, J. D. *Polymer* 1971, **20**, 1071
- 15 Hoffman, J. D. *J. Res. Natl. Bur. Stand. US* 1979, **83A**
- 16 Arridge, R. G. C., Barham, P. J., Farrell, C. J. and Keller, A. J. *Mater. Sci.* 1976, **11**, 788
- 17 Coombes, A. G. and Keller, A. J. *Polym. Sci., Polym. Phys. Edn.* 1979, **17**, 1637
- 18 Grubb, D. T. and Keller A. *Colloid Polym. Sci.* 1978, **256**, 218
- 19 Hill, M. J., Barham, P. J. and Keller, A. *Colloid Polym. Sci.* 1980, **258**, 1023
- 20 Flory, P. J. 'Statistical Mechanics of Chain Molecules', Interscience N.Y. 1969
- 21 Cannon, C. G. private communication
- 22 Grubb, D. T. and Hill, M. J. *J. Cryst. Growth* 1980, **48**, 321
- 23 Cox, H. L. *Br. J. Appl. Phys.* 1952, **3**, 72
- 24 Arridge, R. G. C. and Barham, P. J. *J. Polym. Sci., Polym. Phys. Edn.* 1978, **16**, 1297
- 25 Odajima, A. and Maeda, T. *J. Polym. Sci.* 1966, **C15**, 55
- 26 Wobser, G. and Blasenbury, S. *Colloid Polym. Sci.* 1970, **241**, 985
- 27 Shimanouchi, T., Asahima, M. and Enomoto, S. *J. Polym. Sci.* 1962, **59**, 93